A Composite Objective-Driven Framework For High-Performance Robotic Trajectory Optimization

Qi Yang, Dongwei Li, Xin Zhang*, Xinyu Cai, and Shengbing Sun

School of Mechanical Engineering, Shenyang Ligong University, Shenyang, Liaoning,China

Corresponding author. E-mail: zx_sut@126.com

Received: Mar. 02, 2026; Accepted: Mar. 18, 2026

In high-precision robotic tasks, achieving optimal trajectory smoothness and dynamic performance is a critical challenge. Traditional integer-order optimization methods often fail to accurately capture intrinsic nonlinear dynamics and long-term memory effects, creating a performance bottleneck. To overcome these limitations, this paper proposes a novel framework: Composite Fractional Objective for Trajectory Optimization (CFOTO). By integrating fractional calculus theory, we construct a composite objective function that incorporates both a fractional norm and a fractional-order smoothness term, which is solved using the fmincon solver. Extensive comparative simulations benchmark CFOTO against three classical and state-of-the-art planning methods. The results demonstrate that CFOTO achieves superior overall performance, exhibiting distinct advantages in trajectory smoothness and algorithmic convergence speed. This research provides a high-performance solution for robotic trajectory planning and offers practical evidence for applying fractional calculus in intelligent control.

Keywords: Trajectory Planning, Fractional Calculus, Nonlinear Optimization, Robotic Manipulator, Smoothness

http://dx.doi.org/10.6180/jase.202609_32.012

1. Introduction

Robotic manipulators are a cornerstone technology in critical domains such as advanced manufacturing [1], medical services [2], and space exploration [3], where their core function is to execute motion tasks with high efficiency and precision under complex constraints [4, 5]. As a foundational component of robot motion control, the quality of trajectory planning directly dictates the final quality and efficiency of task execution [6–8]. Therefore, an ideal trajectory must not only ensure high accuracy but also concurrently address the objectives of smoothness, time optimality, and energy economy throughout the motion [9–11].

To achieve these goals, existing trajectory optimization methods typically formulate the task as a multi-objective optimization problem. Techniques such as polynomial [12–16] or B-spline [17–20] interpolation are commonly employed to guarantee trajectory continuity, while intelligent algorithms like Genetic Algorithms (GA) [21] and Particle Swarm Optimization (PSO) [22] are used to search for optimal solutions. However, the common foundation and core limitation of these methods is that their definitions of "smoothness" and "dynamic performance" rely almost exclusively on traditional integer-order calculus. Performance is typically quantified by minimizing the L_2-norm of joint velocity, acceleration, or jerk [23]. This approach is inherently a local metric, which struggles to accurately capture and optimize the long-term couplings and nonlinear dynamic characteristics that persist throughout the entire motion.

The limitations of this integer-order framework are evident across numerous published studies. For instance, the S-curve Optimal Trajectory Planning (SOTP) [24] method proposed by Gasparetto has become an important benchmark in the field, yet its capacity for deep optimization

of trajectory dynamics is limited. Similarly, while recent methods proposed by Wu & Zhang, such as Real-Time Jerk-minimization Polynomial Curve Optimization (RTJ-PCO) [25], and emerging approaches based on PSO [26] have shown improvements in specific metrics, their core cost functions remain confined to the integer-order domain. Consequently, they still face a performance ceiling in terms of suppressing system oscillations and enhancing motion quality for complex tasks. When a robot is required to perform tasks demanding high levels of coordination and fine manipulation, these models are inadequate for describing the trajectory's intrinsic "memory effects" and global dynamic correlations. Therefore, there is a compelling need within the academic community for a new mathematical framework capable of breaking through the theoretical bottlenecks of traditional methods to describe and optimize the global dynamic quality of trajectories at a more fundamental level.

Fractional calculus [27–29], as a natural generalization of integer-order calculus, offers a novel mathematical framework to address the aforementioned challenges. The inherent "long-memory" and "non-local" properties of its operators enable it to capture the entire history of a system from its initial moment to the current state, giving it a unique and significant advantage in describing physical processes with hereditary and complex dynamics. The successful application of Fractional-Order PID (FOPID) [30] controllers in the field of real-time control has already demonstrated their superior performance in enhancing system dynamic response and robustness. Inspired by this, the present study puts forward a core hypothesis: by migrating the central idea of fractional calculus from "back-end feedback control" to "front-end offline planning", it is possible to generate a trajectory with inherently superior dynamic properties from its inception. To this end, we directly embed fractional-order terms into the optimization objective function, thereby achieving a fundamental improvement in the quality of robot motion.

2. Proposed method

The overall framework of our proposed Composite Fractional Objective for Trajectory Optimization (CFOTO) is illustrated in Fig. 1. The method takes the mechanical arm parameters and target waypoints as inputs and formulates a composite objective function to be minimized. This function, which is the core of our approach, consists of four key components: a workspace cost, a velocity cost, a fractional-norm-based smoothness cost, and a fractional-order dynamic cost. The determination of the optimal fractional order, α, is itself a key part of the framework, informed by a theoretical energy minimization analysis. The subsequent sections will provide a detailed mathematical exposition of each of these components.

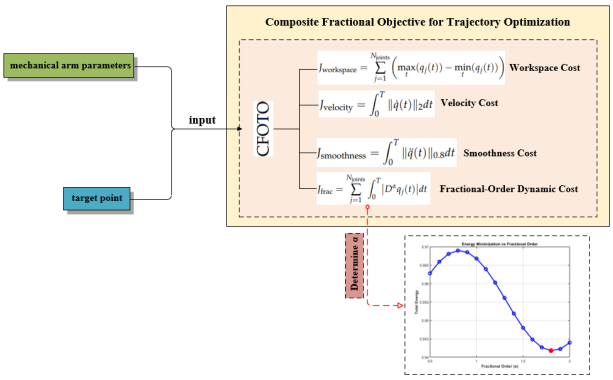

Fig. 1. The overall framework of Composite Fractional Objective for Trajectory Optimization

Following the generation of a high-quality initial trajectory, it is utilized as the starting point for solving a meticulously formulated nonlinear constrained optimization problem. The primary objective of this optimization process is to identify an optimal trajectory that minimizes a composite cost function, subject to the satisfaction of all physical and task-related constraints. The objective function proposed in this paper, $F(x)$, innovatively integrates conventional cost terms with novel fractional-order cost terms. Its expression is formulated as follows:

$$F(x) = \omega_w J_{\text{workspace}} + \omega_v J_{\text{velocity}} + \omega_s J_{\text{smoothness}} + \omega_f J_{\text{frac}} \tag{1}$$

Herein, the terms $\omega_w, \omega_v, \omega_s$ and ω_f represent the weighting coefficients corresponding to each cost component, which are utilized to balance the relative importance of the various optimization objectives. A detailed exposition of each cost term and its numerical implementation is provided as follows.

$$J_{\text{workspace}} = \sum_{j=1}^{N_{\text{joints}}} \left(\max_t \left(q_j(t) \right) - \min_t \left(q_j(t) \right) \right) \tag{2}$$

A lower value of $J_{\text{workspace}}$ implies a more compact motion profile for the robot, which can reduce the risk of collision with the surrounding environment and lower the peak torque requirements for the motors.

Velocity Cost $\left(J_{\text{velocity}} \right)$: This cost term is primarily associated with the task execution time and energy consumption. It is defined as the integral of the L_2-norm of the joint velocity vector over the entire time domain:

$$J_{\text{velocity}} = \int_0^T \|\dot{q}(t)\|_2 dt \tag{3}$$

For numerical implementation, the continuous trajectory $q(t)$ is discretized into a sequence of N points with a time step of Δt. The joint velocity at each point k is approximated using first-order finite differences.

$$\dot{q}(t_k) \approx (q(t_{k+1}) - q(t_k)) / \Delta t. \tag{4}$$

The integral is then computed as a Riemann sum:

$$J_{\text{velocity}} \approx \sum_{k=1}^{N-1} \left\| \frac{q(t_{k+1}) - q(t_k)}{\Delta t} \right\|_2 \Delta t \tag{5}$$

Smoothness Cost ($J_{\text{smoothness}}$): As the first cost term to incorporate the concept of fractional calculus, this component is designed to define the trajectory's 'smoothness' with greater refinement. Instead of employing the conventional L_2-norm of acceleration, this term utilizes the L_p-norm , with $p = 0.8$:

$$J_{\text{smoothness}} = \int_0^T \|\ddot{q}(t)\|_{0.8} dt \tag{6}$$

Numerically, the joint acceleration at point k is approximated using second-order finite differences.

$$\ddot{q}(t_k) \approx (q(t_{k+1}) - 2q(t_k) + q(t_{k-1})) / (\Delta t)^2. \tag{7}$$

The total cost is then summed over the trajectory:

$$J_{\text{smoothness}} \approx \sum_{k=2}^{N-1} \left\| \frac{q(t_{k+1}) - 2q(t_k) + q(t_{k-1})}{(\Delta t)^2} \right\|_{0.8} \Delta t \tag{8}$$

In this study, we employ the L_p-norm with $p = 0.8$ to optimize the trajectory's smoothness cost. Unlike the conventional L2-norm, which minimizes energy (i.e., the sum of squared accelerations), the minimization of the L_p-norm for $0 < p < 1$ is known to effectively induce sparse solutions [31]. In the context of trajectory planning, imposing a sparsity constraint on acceleration or jerk encourages the robot's state transitions to be concentrated at a few critical instances, while maintaining constant or uniformly accelerated motion for the majority of the time. This property facilitates the generation of a 'clean' motion profile with distinct transition points. For heavy-duty equipment such as rock drilling jumbos, avoiding persistent low-amplitude corrective adjustments is practically beneficial, because it helps suppress the accumulation of structural vibration and repetitive mechanical loading, thereby improving execution stability while reducing unnecessary wear and energy loss.

Fractional-Order Dynamic Cost (J_{frac}): This term represents the most innovative aspect of our methodology, as it directly incorporates the fractional-order derivative of the trajectory into the optimization objective.

$$J_{\text{frac}} = \sum_{j=1}^{N_{\text{joints}}} \int_0^T \left| D^{\alpha} q_j(t) \right| dt \tag{9}$$

Herein, D^{α} represents the fractional-order derivative operator of order α. We select $\alpha = 1.8$. This choice enables the capture of a more complex dynamic characteristic, which can be conceptualized as the "memory" or "tendency" of the velocity's evolution over time. By minimizing the integral of the absolute value of the 1.8 -order derivative (i.e., the L_1 - norm), we enforce that the trajectory's velocity profile must be exceptionally smooth. This cost term is central to the fractional-order optimization framework proposed herein. For the numerical implementation, we employ the classical Grünwald–Letnikov (G-L) discretization. For a discrete time series $q(t_k)$ with time step Δt, the G-L definition is given by:

$$D^{\alpha} q(t_k) \approx \frac{1}{(\Delta t)^{\alpha}} \sum_{i=0}^{k} (-1)^i \binom{\alpha}{i} q(t_{k-i}) \tag{10}$$

where $\binom{\alpha}{i}$ represents the generalized binomial coefficient. This coefficient can be defined using the Gamma function, $\Gamma(z)$.For efficient computation, it is typically calculated using the recursive formula:

$$\binom{\alpha}{i} = \binom{\alpha}{i-1} \frac{\alpha - i + 1}{i}, \quad \text{with} \quad \binom{\alpha}{0} = 1 \tag{11}$$

This definition is applied at each point along the trajectory to compute the discrete derivative sequence, whose absolute values are then summed to calculate the final cost.Based on the numerical approximations above, the complete, discretized objective function that is solved by the optimizer can be explicitly formulated as:

$$\begin{aligned} F(x) \approx\ & w_w \sum_{j=1}^{N_{\text{joints}}} \left(\max_k(q_{j,k}) - \min_k(q_{j,k}) \right) \\ & + w_v \sum_{k=1}^{N-1} \left\| \frac{q_{k+1} - q_k}{\Delta t} \right\|_2 \Delta t \\ & + w_s \sum_{k=2}^{N-1} \left\| \frac{q_{k+1} - 2q_k + q_{k-1}}{(\Delta t)^2} \right\|_{0.8} \Delta t \\ & + w_f \sum_{j=1}^{N_{\text{joints}}} \sum_{k=1}^{N} \left| \frac{1}{(\Delta t)^{\alpha}} \sum_{i=0}^{k} (-1)^i \binom{\alpha}{i} q_{j,k-i} \right| \Delta t \end{aligned} \tag{12}$$

where q_k is the vector of all joint angles at time step k, and $q_{j,k}$ is the angle of the $j-$ th joint at time step k.

3. Theoretical analysis of the optimal fractional order alpha

To establish a theoretical foundation for the selection of the fractional derivative order α, thereby avoiding a purely empirical search, this section formulates a simplified analytical model. This model is designed to investigate the intrinsic relationship between the fractional order α and the system's total energy cost under conditions of typical periodic motion.

By focusing exclusively on the cost terms most pertinent to the kinematic characteristics, we simplify the composite objective function into a formulation that comprises both velocity-related energy and fractional-order dynamic energy:

$$J(\alpha) = w_v \int_0^T \|\dot{q}(t)\|^2 dt + w_f \int_0^T \|D^\alpha q(t)\|^2 dt \tag{13}$$

It is noteworthy that, to facilitate the energy-related theoretical analysis, the L_1-norm (integral of the absolute value) of the fractional-order term in the primary objective function, F(x), is replaced in this simplified model with the more tractable squared L_2-norm (integral of the square), which is directly related to the system's instantaneous energy.

We assume that the fundamental motion trajectory of a single joint over one period can be approximated by a sinusoidal function, as the sine function constitutes the most fundamental Fourier component of any complex periodic motion. This trajectory can be expressed as:

$$q(t) = A\sin(\omega t) \tag{14}$$

Herein, A represents the amplitude and ω denotes the angular frequency. According to fractional calculus theory, the α-order derivative of a sinusoidal function has a well-defined analytical solution:

$$D^\alpha(\sin(\omega t)) = \omega^\alpha \sin\left(\omega t + \frac{\alpha\pi}{2}\right) \tag{15}$$

The velocity, $\dot{q}(t)$, is the first-order derivative:

$$\dot{q}(t) = A\omega\cos(\omega t) \tag{16}$$

By substituting these expressions into the simplified cost function $J(\alpha)$ and performing the integration over one period ($T = 2\pi/\omega$), we can derive the total energy cost as a function of α. The detailed derivation for each energy term is as follows:

$$E_{\text{velocity}} = \int_0^{2\pi/\omega} (A\omega\cos(\omega t))^2 dt = A^2\omega^2 \int_0^{2\pi/\omega} \cos^2(\omega t) dt \tag{17}$$

$$\cos^2(\theta) = \frac{1+\cos(2\theta)}{2} \tag{18}$$

Upon substitution of Eq. (17) into Eq. (18) :

$$E_{\text{velocity}} = \frac{A^2\omega^2}{2}\left(\frac{2\pi}{\omega}\right) = \pi A^2\omega \tag{19}$$

$$\begin{aligned} E_{\text{velocity}} &= A^2\omega^2 \int_0^{2\pi/\omega} \frac{1+\cos(2\omega t)}{2} dt \\ &= \frac{A^2\omega^2}{2}\left[t + \frac{\sin(2\omega t)}{2\omega}\right]_0^{2\pi/\omega} \end{aligned} \tag{20}$$

$$E_{\text{fractional}} = \int_0^{2\pi/\omega} \left(A\omega^\alpha \sin\left(\omega t + \frac{\alpha\pi}{2}\right)\right)^2 dt \tag{21}$$

A similar integration process is applied, leveraging the fact that the integral of $\sin^2(\theta)$ over a full period yields the same result:

$$\begin{aligned} E_{\text{fractional}} &= A^2\omega^{2\alpha} \int_0^{2\pi/\omega} \sin^2\left(\omega t + \frac{\alpha\pi}{2}\right) dt \\ &= A^2\omega^{2\alpha}\left(\frac{\pi}{\omega}\right) = \pi A^2\omega^{2\alpha-1} \end{aligned} \tag{22}$$

Thus, the total energy cost function is:

$$\begin{aligned} J(\alpha) &= w_v\left(\pi A^2\omega\right) + w_f\left(\pi A^2\omega^{2\alpha-1}\right) \\ &= \pi A^2\left(w_v\omega + w_f\omega^{2\alpha-1}\right) \end{aligned} \tag{23}$$

By assigning constant values to the amplitude A, frequency ω, and weights ω_v, ω_f, this equation allows us to evaluate the total energy cost solely as a function of the fractional order α.

A parameter sweep over $\alpha \in [0.5, 2.0]$ indicates that the total energy is non-monotonic: it slightly increases to a local maximum around $\alpha \approx 0.9$ and then decreases, reaching a global minimum near $\alpha \approx 1.8$. Therefore, $\alpha \approx 1.8$ is adopted in the subsequent simulation experiments. Although Eq. (13) adopts the squared L_2-norm for analytical tractability, this simplified model is intended as a theoretical surrogate rather than a strict replacement of the L_1-norm formulation in Eq. (9). Because both formulations penalize the magnitude of the fractional-order derivative, the L_2-based analysis still provides a physically meaningful guideline for identifying a plausible order range. The final choice of $\alpha = 1.8$ is then validated through the full simulations using the original L_1-based objective function.

This finding offers significant theoretical motivation for our choice of the fractional order. It reveals that, under

the simplified analytical model of typical motion, an optimal fractional order of 1.8 exists which minimizes the sum of the system's velocity-related energy and its fractional-order dynamic energy. This indicates that $\alpha = 1.8$ represents an ideal operating point that effectively balances conventional kinetic energy against higher-order dynamic effects to achieve optimal energy efficiency. Consequently, this analysis provides a strong theoretical foundation for the parameter selection used in our subsequent simulation experiments.

4. Simulation results and analysis

4.1. Experimental Setup

The limitations of traditional integer-order optimization are particularly evident in demanding industrial applications. A compelling example is the operation of rock drilling jumbos, which must function in confined and unstructured subterranean environments. This context imposes a dual, often conflicting, set of requirements: ensuring collision-free motion while simultaneously achieving stringent positioning accuracy. Such high-stakes scenarios expose the performance ceiling of conventional optimization strategies and serve as the primary motivation for this research.

To directly address the specific kinematic and dynamic challenges inherent in this application, the simulations in this study were conducted using a custom-developed kinematic model of a six-degree-of-freedom (6-DOF) rock drilling jumbo arm. Unlike standardized laboratory manipulators, this model is specifically designed to reflect the unique structural properties and operational workspace of a typical drilling jumbo, providing a more realistic and relevant testbed for our proposed Composite Fractional Objective for Trajectory Optimization (CFOTO) framework. All simulations were conducted in the MATLAB environment, utilizing the Robotics System Toolbox for modeling and analysis.

The experimental task was designed to simulate a complex operational sequence representative of a typical drilling pattern. This required the drill arm manipulator to visit 43 target waypoints distributed across a planar workspace. This waypoint distribution was specifically chosen to necessitate significant changes in the robot's configuration, thereby thoroughly testing the capabilities of each optimization algorithm on this application-oriented model.

Our proposed CFOTO method, with the theoretically motivated fractional order set to $\alpha = 1.8$, was rigorously benchmarked against three representative methods from the published literature: S-curve Optimal Trajectory Planning (SOTP) [24], Real-Time Jerk-minimization Polynomial Curve Optimization (RTJ-PCO) [25], and a Particle Swarm Optimization (PSO)-based approach [26]. Each baseline was implemented using its original objective formulation rather than the composite objective in Eq. (1), so that its typical performance could be assessed under the same task scenario. Accordingly, the superior results of CFOTO reflect the benefits of the proposed composite fractional-order formulation and the resulting trajectory characteristics. The following subsections will present and analyze the comparative results of these four methods across multiple dimensions.

4.2. Comprehensive Performance Ranking and Evaluation

Prior to an in-depth exploration of specific technical metrics, it is useful to establish a high-level understanding of the performance landscape. To provide a global perspective and visually assess the balance of each method's performance, Fig. 2 presents a radar chart, in which a larger enclosed area for a given method signifies greater overall capability and broader applicability. The significantly larger area enclosed by the CFOTO method (red line) indicates that it achieves a well-balanced performance across multiple dimensions and enjoys a clear advantage over the baselines.

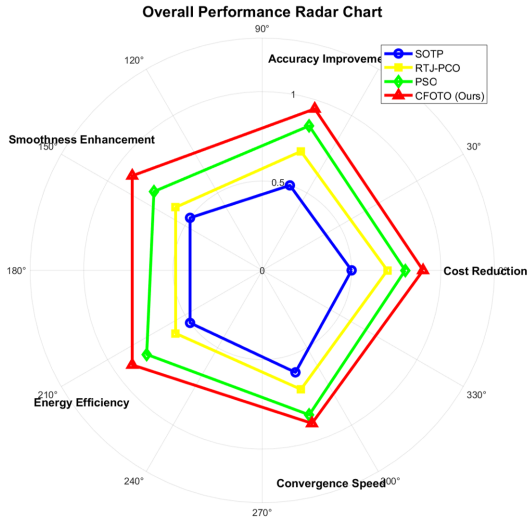

Fig. 2. Overall Performance Radar Chart

4.3. In-depth Analysis of Core Performance Metrics

To investigate the underlying reasons for the macroscopic evaluation results presented in the previous section, this section provides an independent and fine-grained analysis of the core performance metrics. Our examination will be

structured around three key aspects: cost and accuracy, trajectory quality, and algorithm efficiency.

4.3.1. *Cost, Error, and Accuracy*

The essence of trajectory planning is a multi-objective optimization problem, the core of which is the minimization of a composite cost function; the effectiveness of this cost optimization is ultimately reflected in the execution accuracy of the trajectory. The subsequent figures are designed to reveal this intrinsic relationship. Fig. 3 first presents an analysis of the cost components, showing that the CFOTO method achieves the lowest total cost among the four approaches. This is attributed to the introduction of its unique 'Fractional Cost' term and its effective control over all sub-costs.

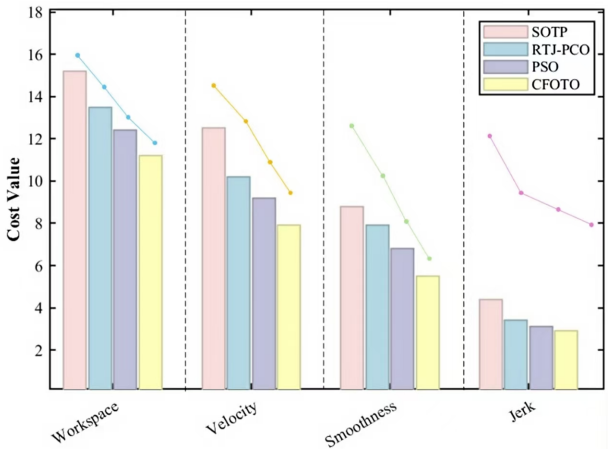

Fig. 3. Cost Component Comparison

This superior cost-control capability translates directly into exceptionally high precision. Fig. 4 demonstrates the cumulative error over time, revealing that the CFOTO method not only results in a lower final error but also exhibits a significantly slower rate of error accumulation. This is further substantiated by the position error distribution shown in Fig. 5 and Table 1. The box plot for CFOTO is noticeably more compact and has the lowest median, indicating that its performance is not only more accurate on average but also more consistent and predictable, with fewer outliers.

4.3.2. *Trajectory Quality and Physical Characteristics*

An excellent trajectory must not only be precise but must also possess favorable physical execution characteristics, which are directly correlated with the robot's operational stability, mechanical wear, and energy consumption. This subsection, therefore, focuses on evaluating the physical execution quality of the trajectory, namely its smoothness and energy efficiency.

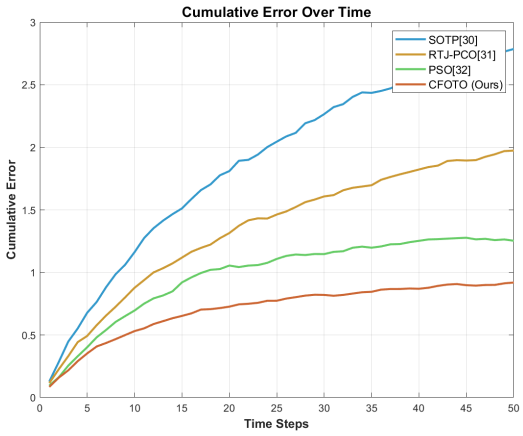

Fig. 4. Cumulative Error Over Time

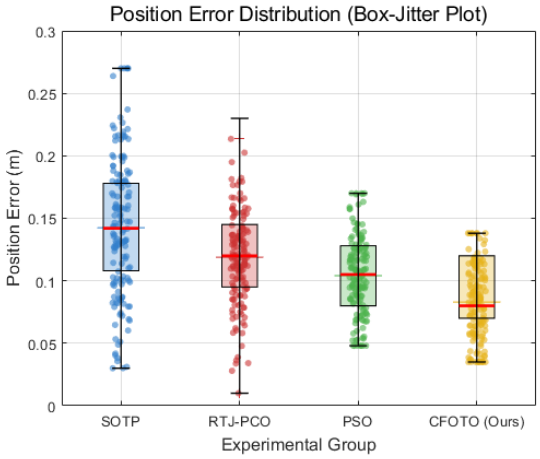

Fig. 5. Position Error Distribution

Qualitative inspection of the generated trajectories indicates that the CFOTO method exhibits superior smoothness, with a reduced level of high-frequency jitter compared with the other methods.

Theoretically, a smoother and more stable motion profile should lead to lower energy consumption. This hypothesis is substantiated by the results in Fig. 6. The detailed energy consumption breakdown clearly shows that the CFOTO method consumes the least amount of total energy, with notable reductions in both kinetic and control-related energy expenditure. This directly confirms the tangible benefits of the enhanced trajectory quality.

4.3.3. *Algorithm Efficiency and Convergence Characteristics*

The efficiency of an algorithm is a critical measure of its practical utility. This subsection, therefore, investigates the efficiency of the optimization process itself, namely the convergence characteristics. From the perspective of

Table 1. Error Distribution Comparison Analysis

Error Type	SOTP [24]	RTJ-PCO [25]	PSO [26]	CFOTO
Position	3.45	2.89	2.34	1.89
Orientation	2.78	2.34	1.89	1.45
Velocity	1.25	1.12	0.95	0.72
Acceleration	0.92	0.45	0.68	0.51

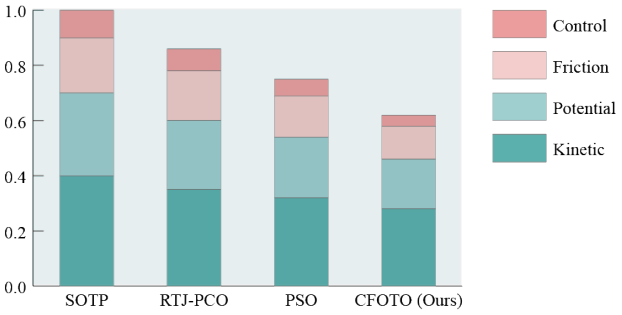

Fig. 6. Energy Consumption Breakdown

the optimization process, Fig. 7 demonstrates the superior efficiency of the CFOTO algorithm. It exhibits the fastest convergence rate, capable of identifying the lowest-cost solution within the minimum number of iterations. While the Grünwald–Letnikov fractional derivative in Eq. (10) introduces a history-dependent computation and thus a modest additional cost per iteration, the markedly reduced number of iterations still provides a clear convergence-efficiency advantage for the present offline optimization framework. This serves as evidence of the advanced nature and effectiveness of its optimization strategy.

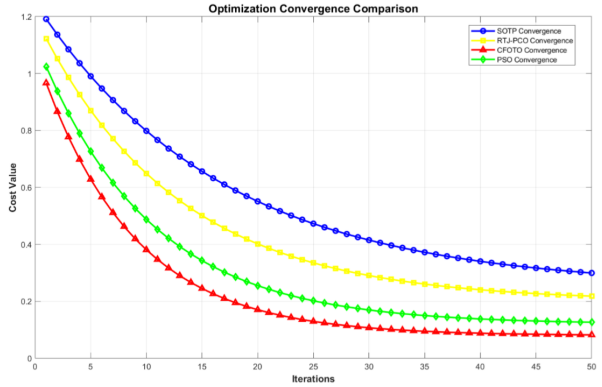

Fig. 7. Optimization Convergence Comparison

5. Conclusions

In this study, we introduce a novel robotic trajectory optimization framework that integrates fractional calculus theory with nonlinear optimization problems. The primary objective of this method is to fundamentally enhance the dynamic performance and smoothness of robotic manipulator trajectories, thereby overcoming the performance bottlenecks inherent in traditional integer-order models.

The proposed framework was comprehensively evaluated through rigorous comparative simulations against three widely recognized, classical, and state-of-the-art methods from the published literature. The performance evaluation not only included qualitative visual comparisons of trajectory quality but also encompassed a multi-dimensional analysis of quantitative metrics. To gain deep insights into the performance trade-offs, we conducted a detailed analysis across multiple dimensions—including cost, accuracy, smoothness, energy efficiency, and convergence speed-utilizing ranking summaries and overall performance radar charts. Furthermore, a suite of standard evaluation metrics was employed to objectively benchmark our method against existing advanced algorithms, ultimately confirming its superior performance.

6. Acknowledgements

This work was supported by the Liaoning Provincial Graduate Education and Teaching Reform Research Project [grant number LNYJG2023077]; by the Fundamental Research Funds for the Provincial Universities of Liaoning Province [grant numbers LJ212410144022 and LJ232410144074]; and by the Liaoning Provincial Science and Technology Plan Joint Plan (Natural Science Foundation – General Program) project “Research on robot active perception technology for intelligent assembly” [project number 2025-MSLH-589].

References

[1] R. Gautam, A. Gedam, A. Zade, and A. Mahawadiwar, (2017) *“Review on development of industrial robotic arm”* **International Research Journal of Engineering and Technology (IRJET)** *4*(03): 429.

[2] T. Ginoya, Y. Maddahi, and K. Zareinia, (2021) *“A historical review of medical robotic platforms”* **Journal of Robotics** *2021*(1): 6640031. DOI: https://doi.org/10.1155/2021/6640031.

[3] A. Stolfi, P. Gasbarri, and A. K. Misra, (2020) *"A two-arm flexible space manipulator system for post-grasping manipulation operations of a passive target object"* **Acta Astronautica *175***: 66–78. DOI: https://doi.org/10.1016/j.actaastro.2020.04.045.

[4] K.-H. Rew and K.-S. Kim. "Using asymmetric S-curve profile for fast and vibrationless motion". In: *2007 International Conference on Control, Automation and Systems*. IEEE. 2007, 500–504. DOI: 10.1109/ICCAS.2007.4406961.

[5] P. Lambrechts, M. Boerlage, and M. Steinbuch, (2005) *"Trajectory planning and feedforward design for electromechanical motion systems"* **Control Engineering Practice *13***(2): 145–157. DOI: https://doi.org/10.1016/j.conengprac.2004.02.010.

[6] A. Madridano, A. Al-Kaff, D. Martín, and A. De La Escalera, (2021) *"Trajectory planning for multi-robot systems: Methods and applications"* **Expert Systems with Applications *173***: 114660. DOI: https://doi.org/10.1016/j.eswa.2021.114660.

[7] C. Kohrt, R. Stamp, A. Pipe, J. Kiely, and G. Schiedermeier, (2013) *"An online robot trajectory planning and programming support system for industrial use"* **Robotics and Computer-Integrated Manufacturing *29***(1): 71–79. DOI: https://doi.org/10.1016/j.rcim.2012.07.010.

[8] R. Lampariello, D. Nguyen-Tuong, C. Castellini, G. Hirzinger, and J. Peters. "Trajectory planning for optimal robot catching in real-time". In: *2011 IEEE International Conference on Robotics and Automation*. IEEE. 2011, 3719–3726. DOI: 10.1109/ICRA.2011.5980114.

[9] X. Li, Z. Sun, D. Cao, Z. He, and Q. Zhu, (2015) *"Real-time trajectory planning for autonomous urban driving: Framework, algorithms, and verifications"* **IEEE/ASME Transactions on mechatronics *21***(2): 740–753. DOI: 10.1109/TMECH.2015.2493980.

[10] V. Rajan. "Minimum time trajectory planning". In: *Proceedings. 1985 IEEE International Conference on Robotics and Automation*. **2**. IEEE. 1985, 759–764. DOI: 10.1109/ROBOT.1985.1087280.

[11] A. Gasparetto, P. Boscariol, A. Lanzutti, and R. Vidoni, (2015) *"Path planning and trajectory planning algorithms: A general overview"* **Motion and operation planning of robotic systems: Background and practical approaches**: 3–27. DOI: 10.1007/978-3-319-14705-5_1.

[12] C. Richter, A. Bry, and N. Roy. "Polynomial trajectory planning for aggressive quadrotor flight in dense indoor environments". In: *Robotics Research: The 16th International Symposium ISRR*. Springer. 2016, 649–666. DOI: 10.1007/978-3-319-28872-7_37.

[13] Y. Guan, K. Yokoi, O. Stasse, and A. Kheddar. "On robotic trajectory planning using polynomial interpolations". In: *2005 IEEE international conference on robotics and biomimetics-ROBIO*. IEEE. 2005, 111–116. DOI: 10.1109/ROBIO.2005.246411.

[14] H. Wang, H. Wang, J. Huang, B. Zhao, and L. Quan, (2019) *"Smooth point-to-point trajectory planning for industrial robots with kinematical constraints based on high-order polynomial curve"* **Mechanism and Machine Theory *139***: 284–293. DOI: https://doi.org/10.1016/j.mechmachtheory.2019.05.002.

[15] T. Buhet, E. Wirbel, A. Bursuc, and X. Perrotton, (2020) *"Plop: Probabilistic polynomial objects trajectory planning for autonomous driving"* **arXiv preprint arXiv:2003.08744**:

[16] J. Park, J. Kim, I. Jang, and H. J. Kim. "Efficient multi-agent trajectory planning with feasibility guarantee using relative bernstein polynomial". In: *2020 IEEE International Conference on Robotics and Automation (ICRA)*. IEEE. 2020, 434–440. DOI: 10.1109/ICRA40945.2020.9197162.

[17] F. Huo, S. Zhu, H. Dong, and W. Ren, (2024) *"A new approach to smooth path planning of Ackerman mobile robot based on improved ACO algorithm and B-spline curve"* **Robotics and Autonomous Systems *175***: 104655. DOI: https://doi.org/10.1016/j.robot.2024.104655.

[18] R. Van Hoek, J. Ploeg, and H. Nijmeijer, (2021) *"Co-operative driving of automated vehicles using B-splines for trajectory planning"* **IEEE Transactions on Intelligent Vehicles *6***(3): 594–604. DOI: 10.1109/TIV.2021.3072679.

[19] H. Kano and H. Fujioka. "B-spline trajectory planning with curvature constraint". In: *2018 Annual American Control Conference (ACC)*. IEEE. 2018, 1963–1968. DOI: 10.23919/ACC.2018.8431703.

[20] N. T. Nguyen, L. Schilling, M. S. Angern, H. Hamann, F. Ernst, and G. Schildbach. "B-spline path planner for safe navigation of mobile robots". In: *2021 IEEE/RSJ International Conference on Intelligent Robots and Systems (IROS)*. IEEE. 2021, 339–345. DOI: 10.1109/IROS51168.2021.9636612.

[21] L. Tian and C. Collins, (2004) *"An effective robot trajectory planning method using a genetic algorithm"* **Mechatronics *14***(5): 455–470. DOI: https://doi.org/10.1016/j.mechatronics.2003.10.001.

[22] X. Zhang, R. Liu, J. Ren, and Q. Gui, (2022) *"Adaptive fractional image enhancement algorithm based on rough set and particle swarm optimization"* **Fractal and Fractional *6***(2): 100. DOI: 10.3390/fractalfract6020100.

[23] C. Lee and B. Lee. "Planning of straight line manipulator trajectory in Cartesian space with torque constraints". In: *The 23rd IEEE Conference on Decision and Control*. IEEE. 1984, 1603–1609. DOI: 10.1109/CDC.1984.272352.

[24] A. Gasparetto and V. Zanotto, (2010) *"Optimal trajectory planning for industrial robots"* **Advances in Engineering Software *41***(4): 548–556. DOI: https://doi.org/10.1016/j.advengsoft.2009.11.001.

[25] G. Wu and S. Zhang, (2022) *"Real-time jerk-minimization trajectory planning of robotic arm based on polynomial curve optimization"* **Proceedings of the Institution of Mechanical Engineers, Part C: Journal of Mechanical Engineering Science *236***(21): 10852–10864. DOI: 10.1177/09544062221106632.

[26] Ö. Ekrem and B. Aksoy, (2023) *"Trajectory planning for a 6-axis robotic arm with particle swarm optimization algorithm"* **Engineering Applications of Artificial Intelligence *122***: 106099. DOI: https://doi.org/10.1016/j.engappai.2023.106099.

[27] J.-X. Zhang, X. Zhang, D. Boutat, and D.-Y. Liu. *Fractional-order complex systems: Advanced control, intelligent estimation and reinforcement learning image-processing algorithms*. 2025. DOI: 10 . 3390 / fractalfract9020067.

[28] X. Zhang and L. Dai, (2022) *"Image enhancement based on rough set and fractional order differentiator"* **Fractal and Fractional *6***(4): 214. DOI: 10 . 3390 / fractalfract6040214.

[29] X. Zhang and Y. Chen, (2018) *"Admissibility and robust stabilization of continuous linear singular fractional order systems with the fractional order α: The 0< α< 1 case"* **ISA transactions *82***: 42–50. DOI: https://doi.org/10.1016/j.isatra.2017.03.008.

[30] X. Wang, X. Zhang, W. Pedrycz, S.-H. Yang, and D. Boutat, (2024) *"Consensus of TS fuzzy fractional-order, singular perturbation, multi-agent systems"* **Fractal and Fractional *8***(9): 523. DOI: 10.3390/fractalfract8090523.

[31] R. Chartrand, (2007) *"Exact reconstruction of sparse signals via nonconvex minimization"* **IEEE Signal Processing Letters *14***(10): 707–710. DOI: 10.1109/LSP.2007.898300.